Analysis of small spacecraft Mars aerocapture through a single-event drag modulation

Tobia Armando La Marca[1,a] *, Giorgio Isoletta[2,b] and Michele Grassi[2,c]

[1]Scuola Superiore Meridionale, Largo San Marcellino 10, 80138 Naples, Italy

[2]Department of Industrial Engineering, University of Naples "Federico II", Piazzale Tecchio 80, 80125 Naples, Italy

[a] tobiaarmando.lamarca-ssm@unina.it, [b] giorgio.isoletta@unina.it, [c] michele.grassi@unina.it

Keywords: Aerocapture, Drag Modulation, Mars Exploration, Small Spacecraft

Abstract. In the last years, the scientific interest in Mars exploration has become more and more relevant, driving the development of technologies aimed at improving the current capabilities to land scientific payloads or to insert probes into stable orbits around the planet. In this framework, the use of low-cost small satellites could represent an advantageous solution for both the mission scenarios. In planetary exploration, the aerocapture manoeuvre is considered a promising technique to overcome the limits imposed by specific volume and mass ratio constraints on the design of the propulsion system. Based on these premises, this work focuses on the 2D aerocapture manoeuvre of a small spacecraft equipped with a Deployable Heat Shield (DHS). Specifically, the analysis aims at assessing the aerocapture manoeuvre feasibility exploiting a single shield surface variation.

Introduction

The aerocapture is an aero-assisted manoeuvre to transfer a vehicle from a hyperbolic orbit to a closed one at lower energy, by exploiting the aerodynamic drag force through a single atmospheric passage with properly designed decelerators, such as DHS, drag skirt or inflatable drag devices. Once out of the atmosphere, the spacecraft performs a subsequent Pericenter Raise Manoeuvre (PRM) to avoid repeated atmospheric passages and stabilize the spacecraft on a scientific orbit or on a parking orbit, ready for suppletive Post-Aerocapture Manoeuvres (PAM). If compared to a purely propulsive orbit injection (OI), the aerocapture manoeuvre allows to drastically increase the delivered mass payload thanks to the propellant savings and the smaller weight of the aerodynamic decelerators compared to the propellant needed for propulsive OI. The reduction of the propellant mass decreases the costs per kg of payload, thus enabling or enhancing many potential planetary mission profiles [1]. Moreover, the aerocapture benefits of inherent reduction of the manoeuvring time with respect to the aerobraking manoeuvre, which instead exploits multiple atmospheric passages for depleting the right amount of energy to reach the final orbit. Although the consensus of recent studies about the possibility to use aerocapture for science mission at Titan, Mars and possibly Venus [2], it has never been implemented to date because of environmental and object related uncertainties, e.g., the limited knowledge of the local atmospheric density and/or the lack of real-time navigation data. However, both the growing scientific interest in Mars exploration and the technological readiness acquired in atmospheric flights during the last decades motivate further investigations on Mars aerocapture. This contribution specifically focuses on the aerocapture technique for a small satellite equipped with a DHS, exploiting a single-event drag modulation. The aerocapture has been studied from a purely dynamical point of view, and a multiparametric analysis has been carried out to identify suitable aerocapture corridors. The results of the single-event drag modulation strategy are compared with the outcomes of fixed shield aperture strategy to assess the benefits of this technique in terms of number and characteristics of possible solutions.

Finally, the conductive thermal heat at the pericenter has been estimated to evaluate the thermodynamical loads the spacecraft will encounter during the atmospheric crossing.

Methodology

The present work analyses the aerocapture manoeuvre of a spacecraft initially moving on a hyperbolic approaching trajectory, resulting from a patched conics approximation of the Earth-to-Mars interplanetary transfer. According to this construction, the spacecraft dynamics can be modelled as a two-body problem. The trajectory is then propagated up to the Mars Atmospheric Interface (AI), usually set to 150 km. Once the spacecraft crosses the atmosphere, the drag perturbs the motion as according to the following equation:

$$\ddot{\vec{r}} + \frac{\mu_{Mars}}{r^3} \vec{r} = \vec{a_d} \tag{1}$$

where $\vec{r}$ is the spacecraft position vector in a 2D reference frame centred in Mars, μ_{Mars} is the planetary standard gravitational parameter, while $\vec{a_d}$ the atmospheric drag perturbing acceleration modelled as:

$$\vec{a_d} >". \frac{2}{3}\frac{\rho}{\beta} v\vec{v} \tag{2}$$

In Eq. 2, ρ is the atmospheric density, $\vec{v}$ is the spacecraft velocity vector relative to the atmosphere, v is its module and β is the ballistic coefficient defined as $\beta = \frac{m}{C_D S}$, being C_D the drag coefficient, S the shield cross-section and m the spacecraft mass. The velocity variation produced by the aerodynamic deceleration, Δv_{drag}, has been computed as the difference of the velocity at the pericentres of the arrival hyperbolic trajectory and the elliptical one obtained after the atmospheric crossing. Moreover, the impulsive burn Δv_{PRM} to circularize the elliptical exit orbit has been computed as a Hohmannian manoeuvre executed at the ellipse apoapsis as:

$$\Delta v_{PRM} = \sqrt{\frac{\mu_{Mars}}{r_a}} - \sqrt{\mu_{Mars}(\frac{2}{r_a} - \frac{1}{a_{exit}})} \tag{3}$$

where r_a and a_{exit} are respectively the apocenter and the semi-major axis of the elliptical orbit. Finally, the Sutton and Graves [3] semi-empirical relation for stagnation-point convective heat rate has been employed to quantify the thermal conductive heat rate in W/m^2:

$$\dot{q}_c = K_m \left(\frac{\rho}{R_N}\right)^{0.5} v^3 \tag{4}$$

in which K_m is the Mars atmospheric conductive constant (1.898×10^{-4} kg$^{0.5}$/m) and R_N is the shield nosecone radius. Results are then converted into W/cm^2 to compare them with literature ones.

Results

Results here provided refer to spacecraft characteristics in [4] (and references therein). The spacecraft of *m = 150 kg* is equipped with a DHS providing a maximum surface extension of S_{max} = 7.065 m^2 and a R_N of 0.6 m. All the simulations have been conducted assuming the possibility of changing the shield surface after the spacecraft transit at the pericenter of the arrival trajectory. Several dynamics conditions have been evaluated, resulting from the combination of arrival velocities (v_∞ = 2, 3, 5 km/s), Keplerian arrival pericenters (h_p = 70,75,80,85,90 km) and trigger altitudes for the ballistic coefficient variation (h_{tr}), supposing two different possible values of β respectively equal to 2β and 3β, and analyzing all the trigger altitudes from the Keplerian pericenter up to the aerodynamic interface, with step of 5 km. Moreover, results here reported

refers to the density nominal condition for September 1st, 2031, of the Mars Global Reference Atmospheric Model (Mars-GRAM) [4], and to a $C_D = 1$. Figure 1 shows the apocentric altitude h_a and eccentricity e_{exit} of the orbit obtained after the atmospheric passage as function of h_{tr} and β for $v_\infty = 3km/s$, while Table 1 lists the values of $\dot{q}_c$ at the pericenter, Δv_{drag} and Δv_{PRM} for some of the most relevant settings. In all the figures, dashed lines represent the solution achievable with the nominal (constant) ballistic coefficient.
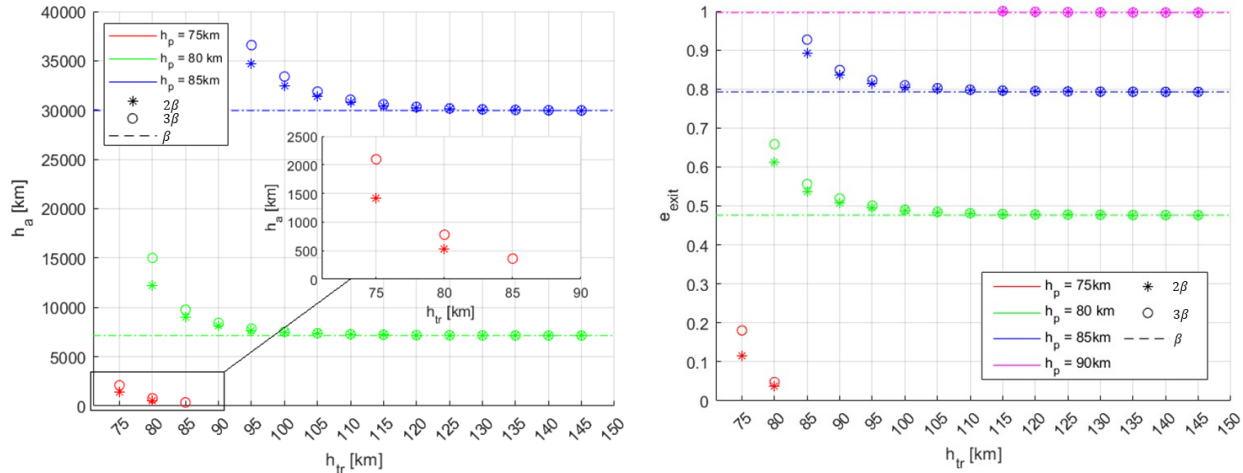

Figure 1 – exit orbit h_a and e_{exit} as function of h_{tr} for different h_p, β and v_∞ = 3 km/s

Table 1 - Most relevant results for v_∞ = 3 km/s

h_p [km]	h_{tr} [km]	$\Delta v_{drag,2\beta}$ [km/s]	$\Delta v_{drag,3\beta}$[km/s]	$\Delta v_{PRM,2\beta}$ [km/s]	$\Delta v_{PRM,3\beta}$ [km/s]	$\dot{q}_c$ [W/cm^2]
75	75	-1.607	-1.508	0.253	0.336	10.21
75	85	//	-1.780	//	0.0802	10.21
80	80	-0.906	-0.843	0.657	0.665	10.15
80	110	-1.086	-1.084	0.598	0.599	10.15
85	95	-0.645	-0.631	0.629	0.620	9.035
85	110	-0.669	-0.668	0.638	0.637	9.035

As expected, the largest variation of the exit orbit parameters is obtained when the ballistic coefficient modulation is triggered soon after the transit of the spacecraft at the pericenter. In particular, because of the larger density values encountered during the atmospheric crossing, the smaller is the h_p, the more circular is the exit orbit (i.e. the smaller are both e_{exit} and h_a). In turn, up to $h_p = 80km$, Δv_{PRM} reduces with increasing h_{tr}, because of the larger amount of time spent with S_{max} at low altitudes, On the other hand, $\dot{q}_c$ values at the pericenters are in line with those expected from the literature [3], showing a small variation with h_p. Finally, an important result is that, thanks to the variation of β, it is possible to have solutions also at pericenter altitude where we have no solutions with the nominal β (i.e. 75 km), that are of high interest due to the possibility to reduce the eccentricity of the exit orbits. However, no solutions have been obtained for h_p smaller than 75 km or larger than 85 km. To better understand the range of aerocapture solutions, in Fig. 2 the results for $v_\infty = 2$ and 5 km/s are depicted, while Tab.2 focuses on most relevant results obtained.

When the hyperbolic speed is of 5 km/s, it is possible to have solution only for $h_p = 75$ km. On the contrary, when the satellite arrival speed is smaller, solutions have been obtained only for h_p higher than 75km, since the atmospheric drag at those altitudes is considerably smaller. However, as previously described, the final h_a is again severely affected by the h_p and v_∞ values.
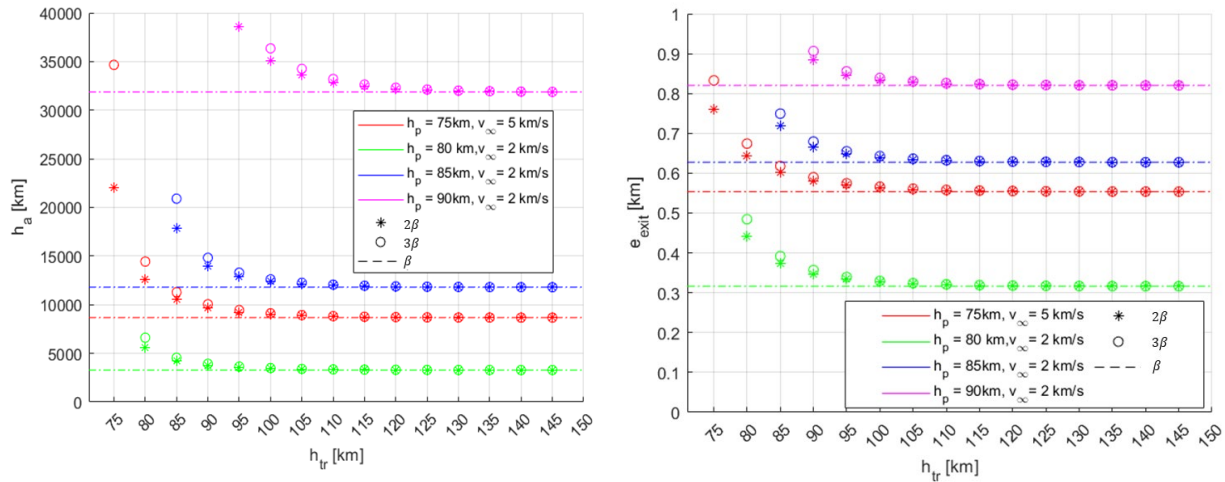
Figure 2 - exit orbit h_a and e_{exit} as function of h_{tr} for different h_p, β and v_∞ = 2 and 5 km/s

Table 2 - Most relevant results for v_∞ = 2 and 5 km/s

h_P [km]	h_{tr} [km]	$\Delta v_{drag,2\beta}$ [km/s]	$\Delta v_{drag,3\beta}$[km/s]	$\Delta v_{PRM,2\beta}$ [km/s]	$\Delta v_{PRM,3\beta}$ [km/s]	$\dot{q}_c$ [W/cm^2]
75	75	-1.43	-1.34	0.661	0.627	15.72
75	110	-1.71	-1.71	0.626	0.627	15.72
80	80	-0.94	-0.88	0.553	0.583	8.74
80	110	-1.12	-1.12	0.442	0.443	8.74
90	95	-0.40	-0.38	0.614	0.606	6.72
90	120	-0.42	-0.42	0.633	0.633	6.72

Conclusions

This work presents an analysis of a single-event aerocapture manoeuvre for a small spacecraft equipped with a DHS. Results confirm the increasing number of solutions achievable with a ballistic coefficient modulation, although a strong dependency on the arrival conditions emerges. Additionally, aerocapture enables some otherwise unattainable exit orbits. For relatively high arrival speed, the atmospheric aerocapture corridor shortens in such a way to suggest further investigation of possible control techniques for a finer modulation of the deployable shield aperture. Thus, future development will focus on 3D aerocapture analysis with the definition of a deployable shield modulation logic.

References

[1]   J. L. Hall, M. A. Noca, and R. W. Bailey, "Cost-Benefit Analysis of the Aerocapture Mission Set," *J Spacecr Rockets*, vol. 42, no. 2, pp. 309–320, Mar. 2005. https://doi.org/10.2514/1.4118

[2]   T. R. Spilker *et al.*, "Qualitative Assessment of Aerocapture and Applications to Future Missions," *J Spacecr Rockets*, vol. 56, no. 2, pp. 536–545, Nov. 2018. https://doi.org/10.2514/1.A34056

[3]   Z. R. Putnam and R. D. Braun, "Drag-Modulation Flight-Control System Options for Planetary Aerocapture," *J Spacecr Rockets*, vol. 51, no. 1, pp. 139–150, Aug. 2013. https://doi.org/10.2514/1.A32589

[4]   G. Isoletta, M. Grassi, E. Fantino, D. de la Torre Sangrà, and J. Peláez, "Feasibility Study of Aerocapture at Mars with an Innovative Deployable Heat Shield," *J Spacecr Rockets*, vol. 58, no. 6, pp. 1752–1761, Jun. 2021. https://doi.org/10.2514/1.A35016